

H. Wulff

Universität Greifswald,  
Institut für Chemie und Biochemie



## Röntgenographische Charakterisierung von plasmagestützt abgeschiedenen ITO-Schichten



Mühlleithen, 18.-20. März 2003

# Gliederung

## 1. Einführung

## 2. Angewandte Methoden

Röntgendiffraktometrie im streifenden Einfall (GIXRD)

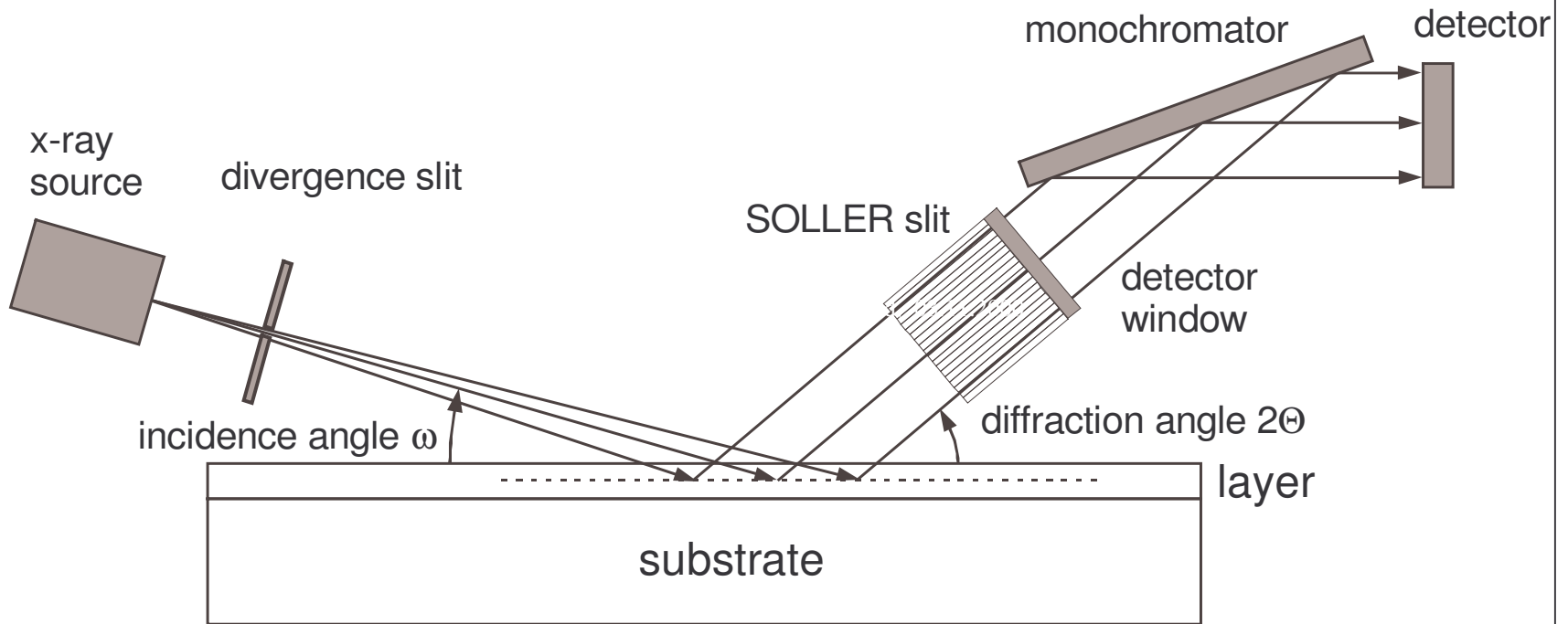
Röntgenreflektometrie (GIXR)

## 3. Ergebnisse

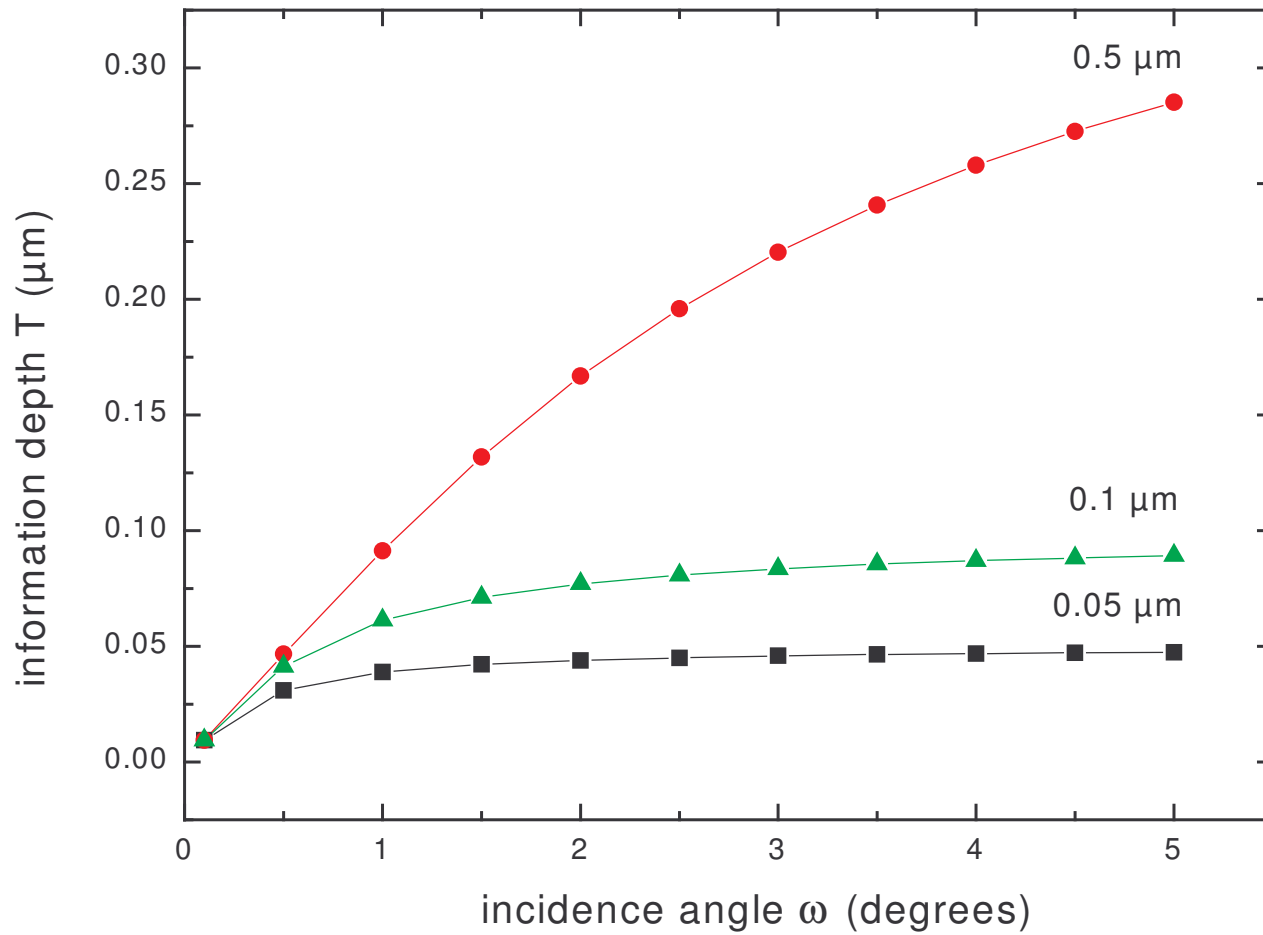
- Einfluß von Sauerstoff und Bias-Spannungen während der Schichtabscheidung
- Temperatur- und zeitaufgelöste Untersuchung von ITO-Schichten (Diffusion, Kristallwachstum)

## 4. Zusammenfassung

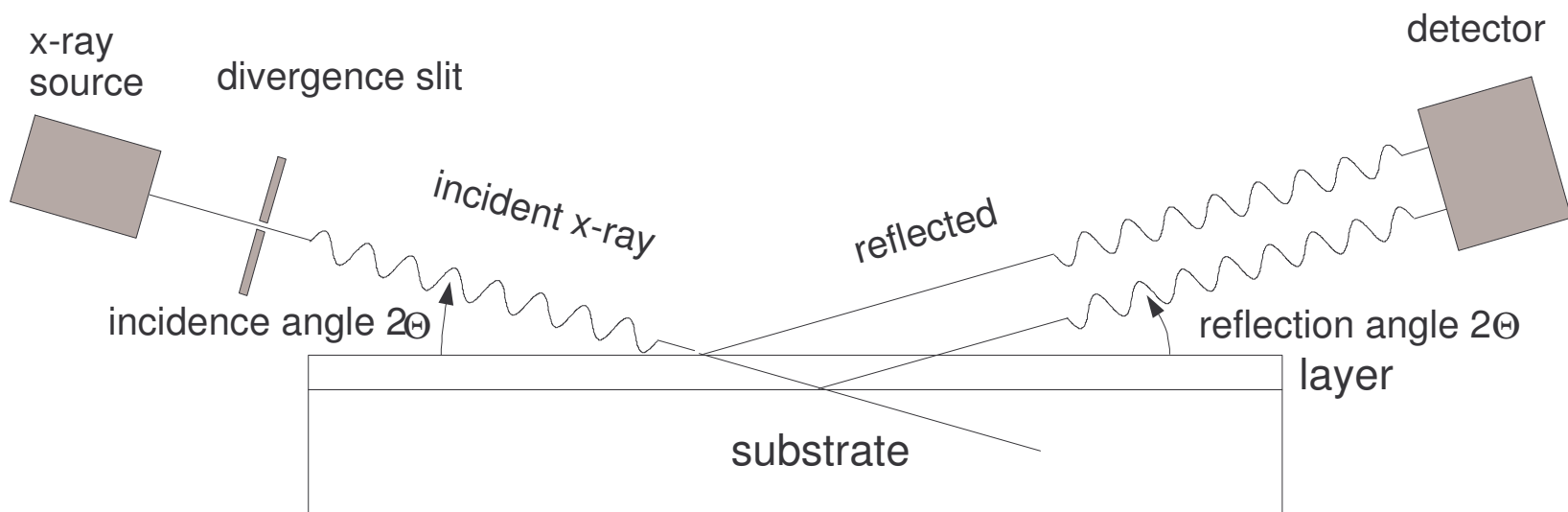
<b>Film property</b>	<b>X-ray method</b>	<b>Alternatives</b>
phase composition	<b>GIXRD</b> : Bragg angle, intensity	TEM
chemical composition (mixed crystals)	<b>GIXRD</b> : Bragg angle	EDX, XPS, RBS
macrostress	<b>GIXRD</b> : Bragg angle	substrate curvature, laser optics
grain size	<b>GIXRD</b> : line profile, line width	TEM, SEM
microstrain	<b>GIXRD</b> : line profile	
preferred orientation	<b>GIXRD</b> : intensity, polfigure	
crystal structure	<b>GIXRD</b> : Rietveld analysis, structure refinement	
thickness	<b>GIXRD</b> : intensity <b>GIXR</b> : Kiessig fringes	interferometry, ellipsometry, TEM
density	<b>GIXR</b> : critical angle of total reflection	ellipsometry
surface roughness interface roughness	<b>GIXR</b> : amplitude of Kiessig fringes	SEM, ellipsometry, AFM
diffusion behavior	in situ <b>GIXRD</b> , thermal and time resolved: intensity	SIMS, AES, combined with sputtering
crystallization rate	in situ <b>GIXRD</b> , thermal and time resolved: intensity	



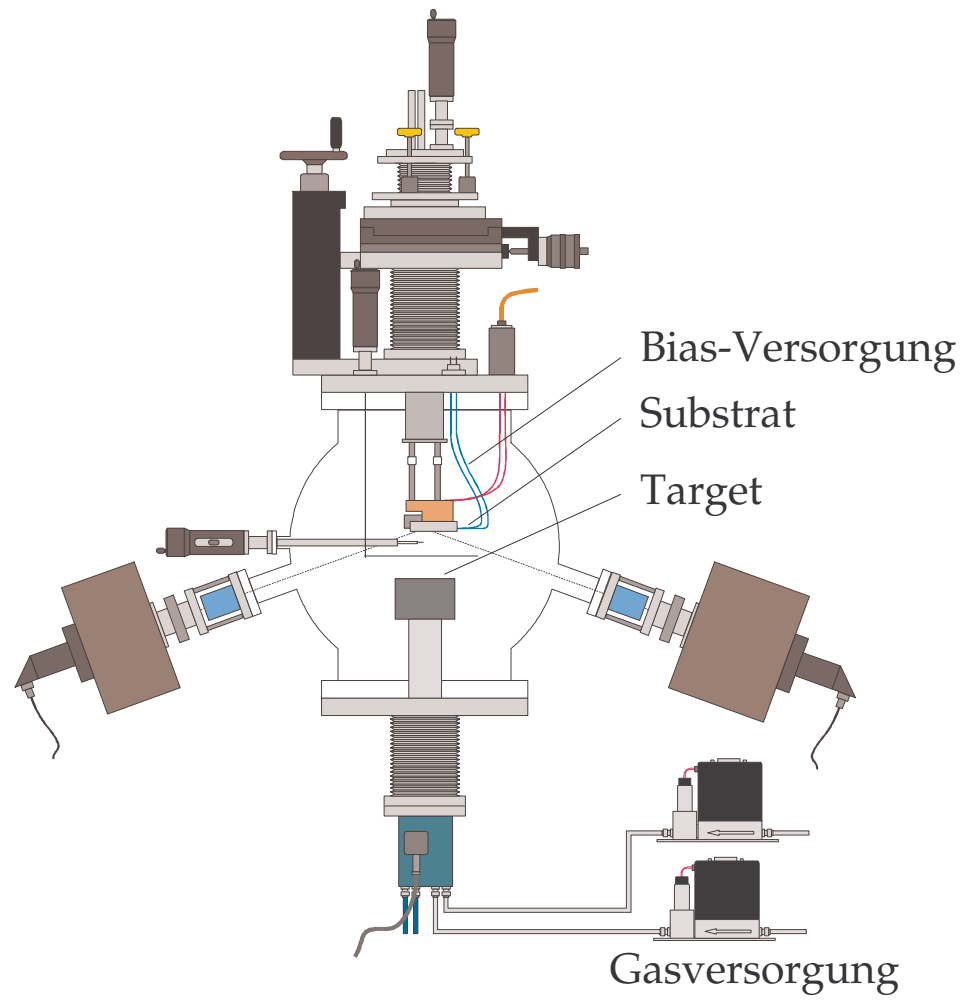
Schematic diagram of grazing incidence X-ray diffractometry (GIXRD),  
 $2\theta$  Bragg angle,  $\omega$  angle of incidence



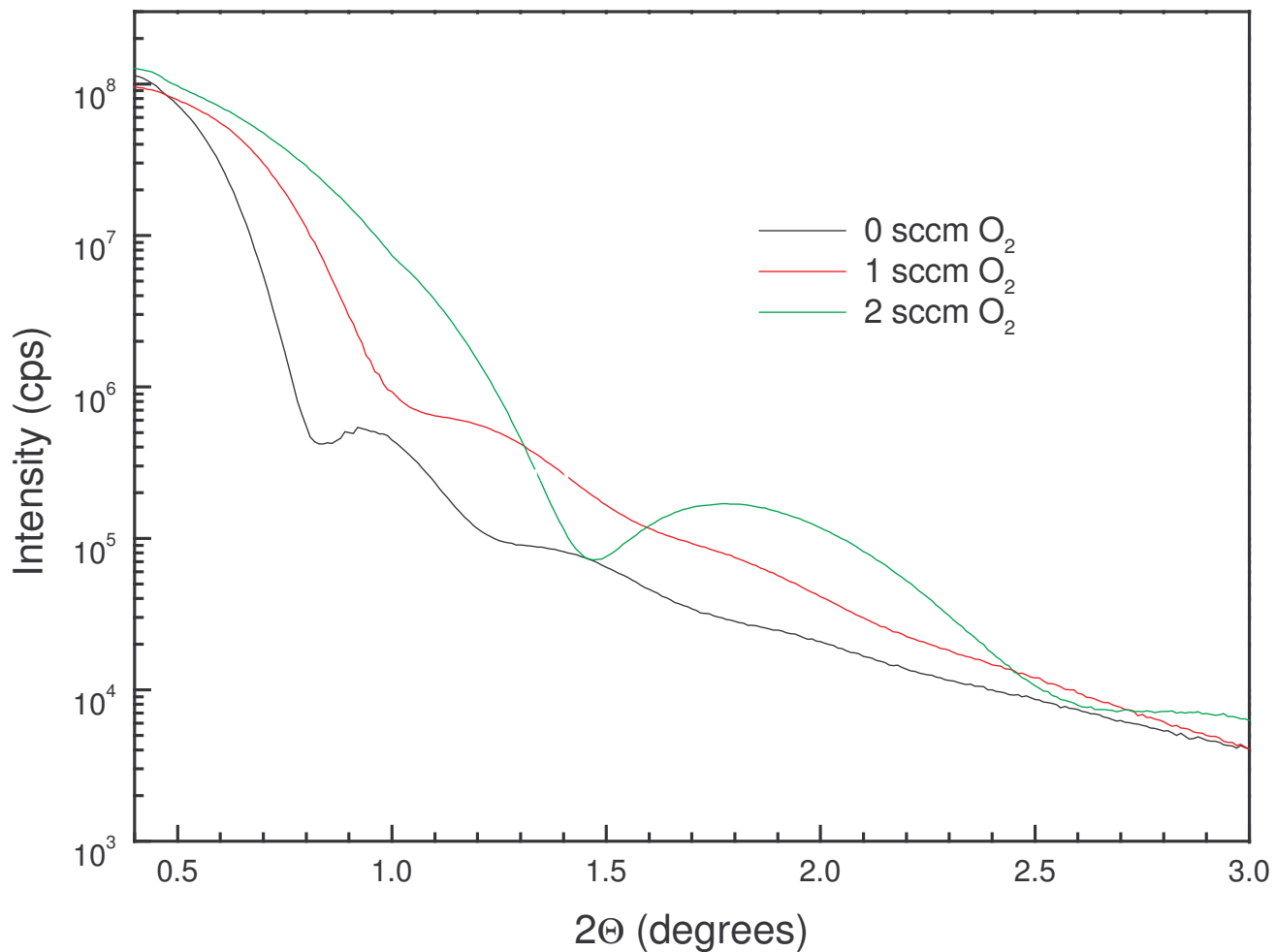
Information depth of Cu K $\alpha$  radiation depending on incidence angles, calculated for 0.05, 0.1 and 0.5 $\mu$ m thick In films



Schematic diagram of grazing incidence X-ray reflectometry (GIXR)



*DC-Magnetron Sputtering System*

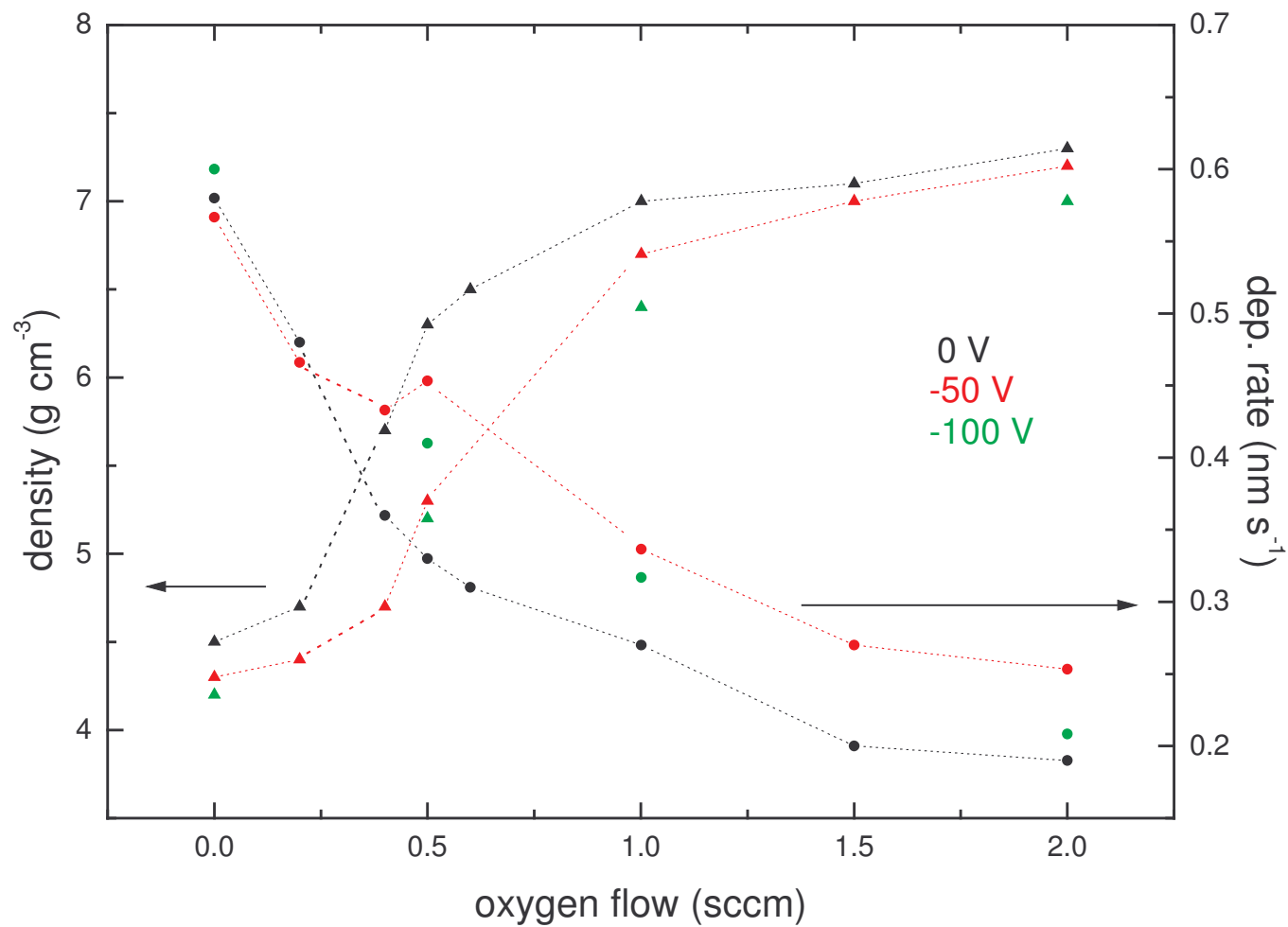


GIXR measurements of films deposited at different oxygen flows,  $U_{\text{sub}} = 0$  V:

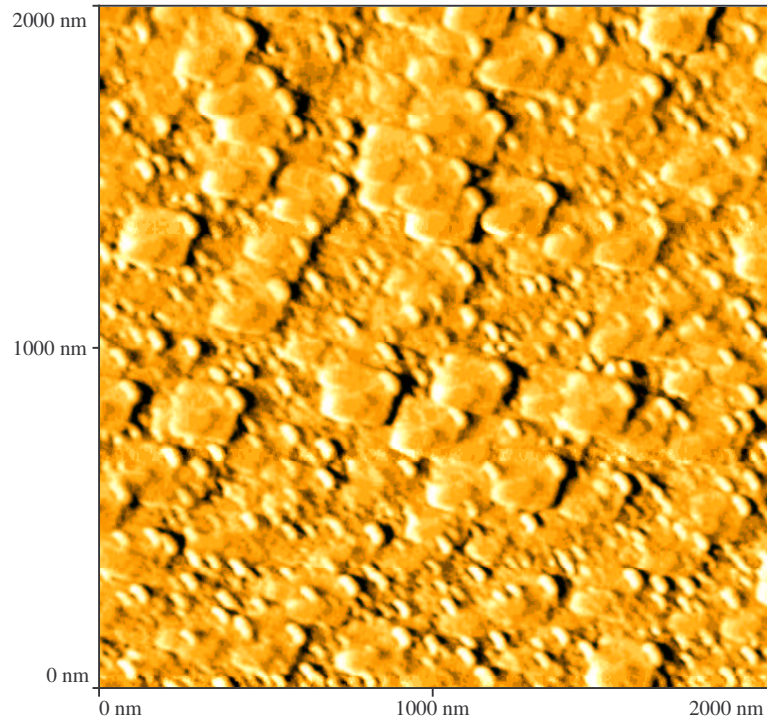
0 sccm  $O_2$ , thickness 15.1 nm, roughness 1.52 nm;

1 sccm  $O_2$ , thickness 11.5 nm, roughness 0.98 nm;

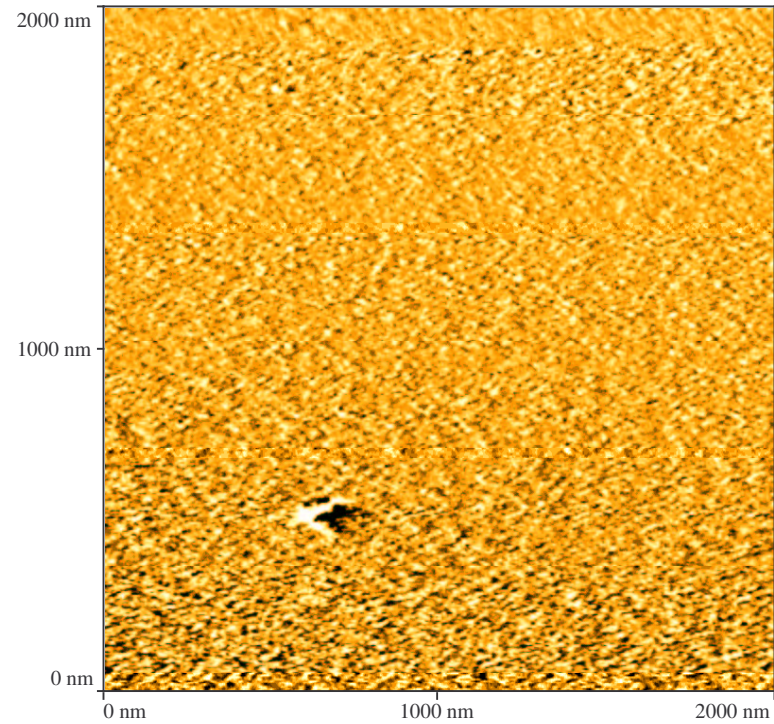
2 sccm  $O_2$ , thickness 7.1 nm, roughness 0.75 nm



Density (▲) and deposition rate (●) of samples deposited at 0V, -50V and -100V substrate voltage vs. oxygen flow

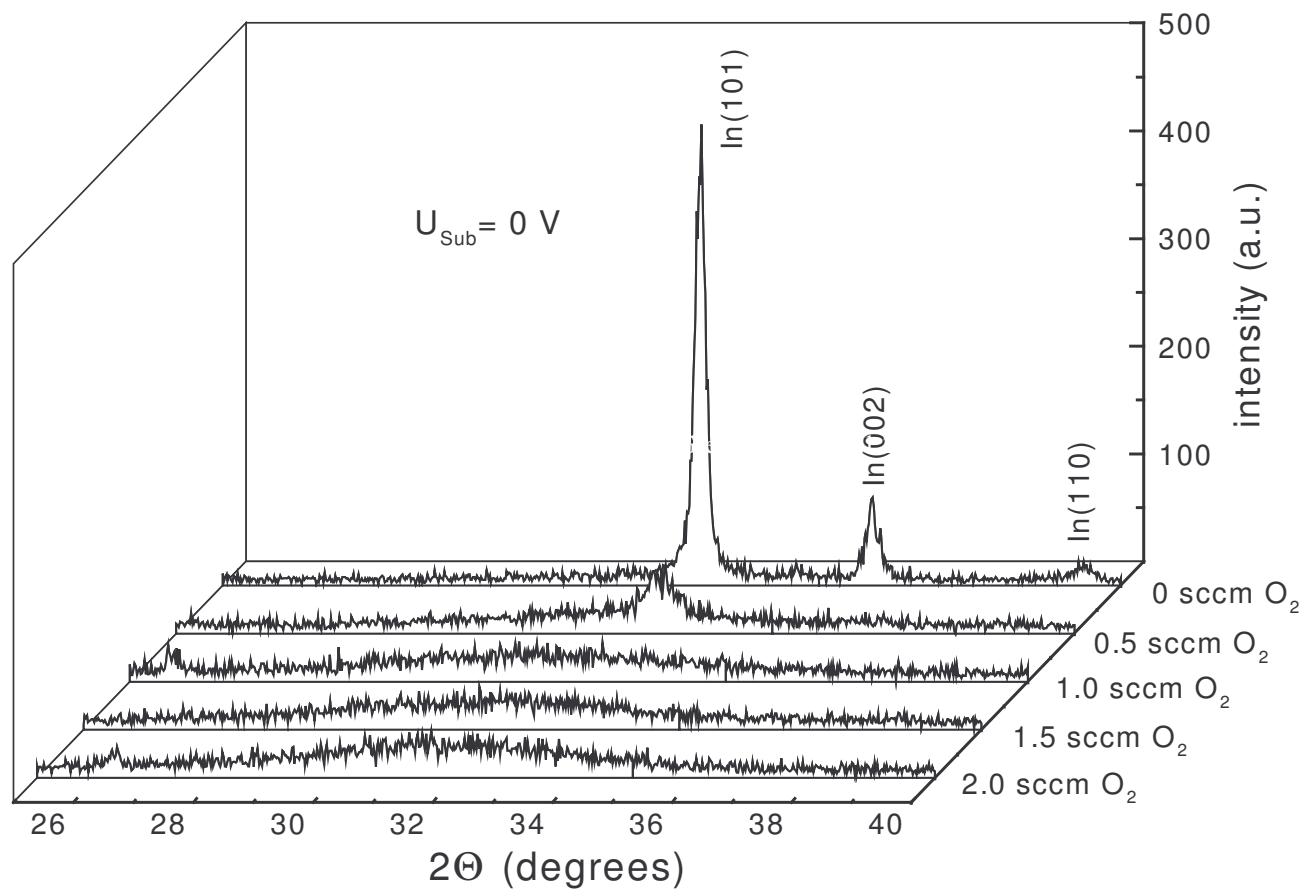


a)

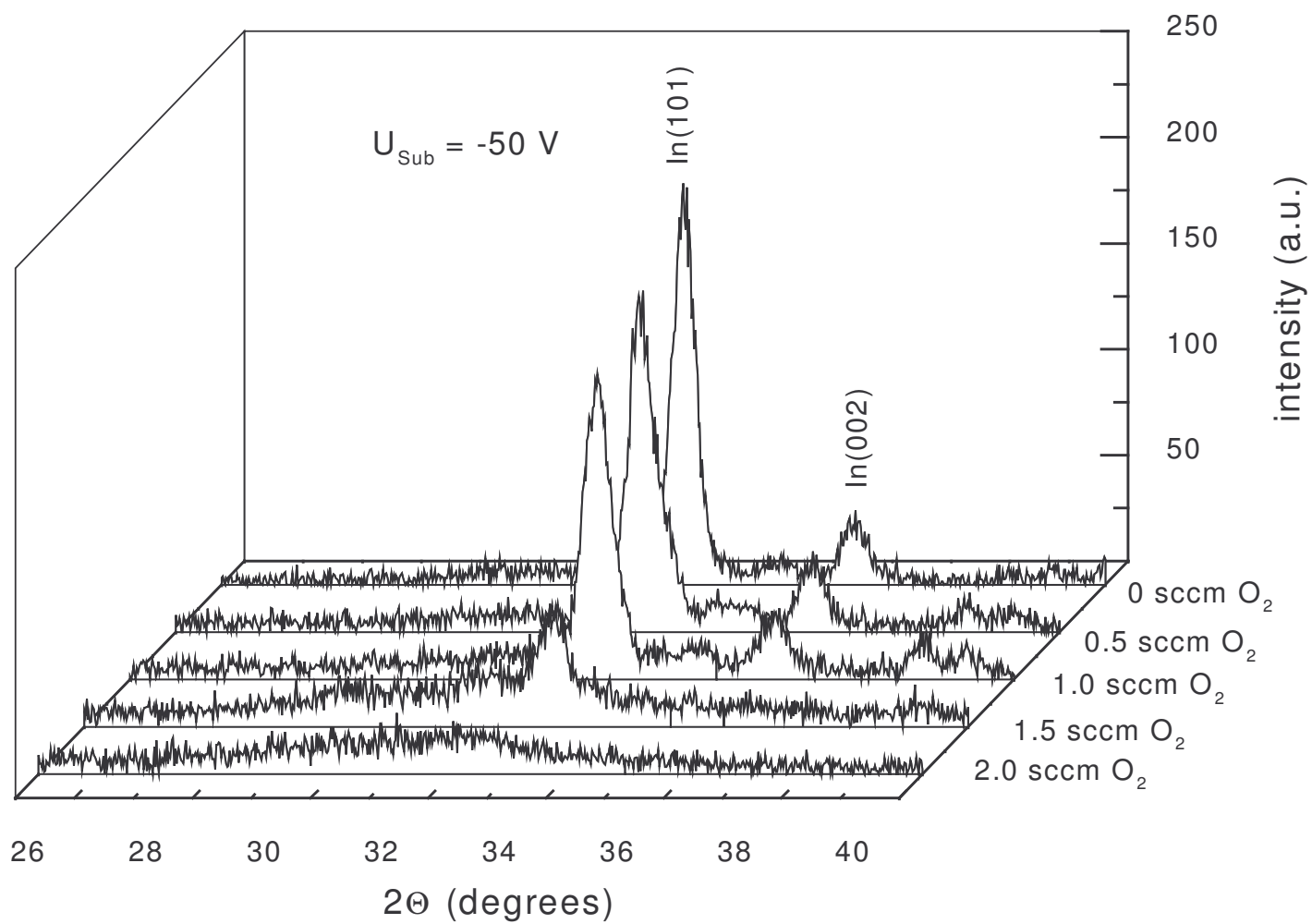


b)

AFM micrographs , samples deposited (a) without  $O_2$  and (b) at 1.5 sccm  $O_2$ ;  
 $U_{sub} = 0$  V, deposition time 30 s



Diffraction patterns of ITO-films deposited at different oxygen flows,  $U_{\text{sub}} = 0 \text{ V}$



Diffraction patterns of films deposited at different oxygen flows,  $U_{\text{sub}} = -50 \text{ V}$

## Röntgenprofilanalyse

$$h(x) = \int f(y) * g(x - y) dy$$

$$F(L) = \frac{H(L)}{G(L)} \quad \text{STOKES Methode}$$

F(L), H(L) G(L) sind die Fouriertransformierten von f(x), h(x) und g(x)  
Normiert auf  $F(0) = H(0) = G(0) = 1$

$$A(L) = a_p(L) * a_s(L) * a_d(L)$$

$$A(L) = \exp(-L/T) * \exp(-K \langle \varepsilon^2 \rangle L^2) * \exp(-B \ln(L_0/L) L^2)$$

$$\text{und } -\ln A(L) = L/T + \langle K \langle \varepsilon^2 \rangle + B \ln(L_0/L) \rangle L^2$$

$$L = n * d(hkl)$$

Meßlänge in Richtung des Beugungsvektors

$$T = T(hkl)$$

effektive Teilchengröße

$$B = B(hkl)$$

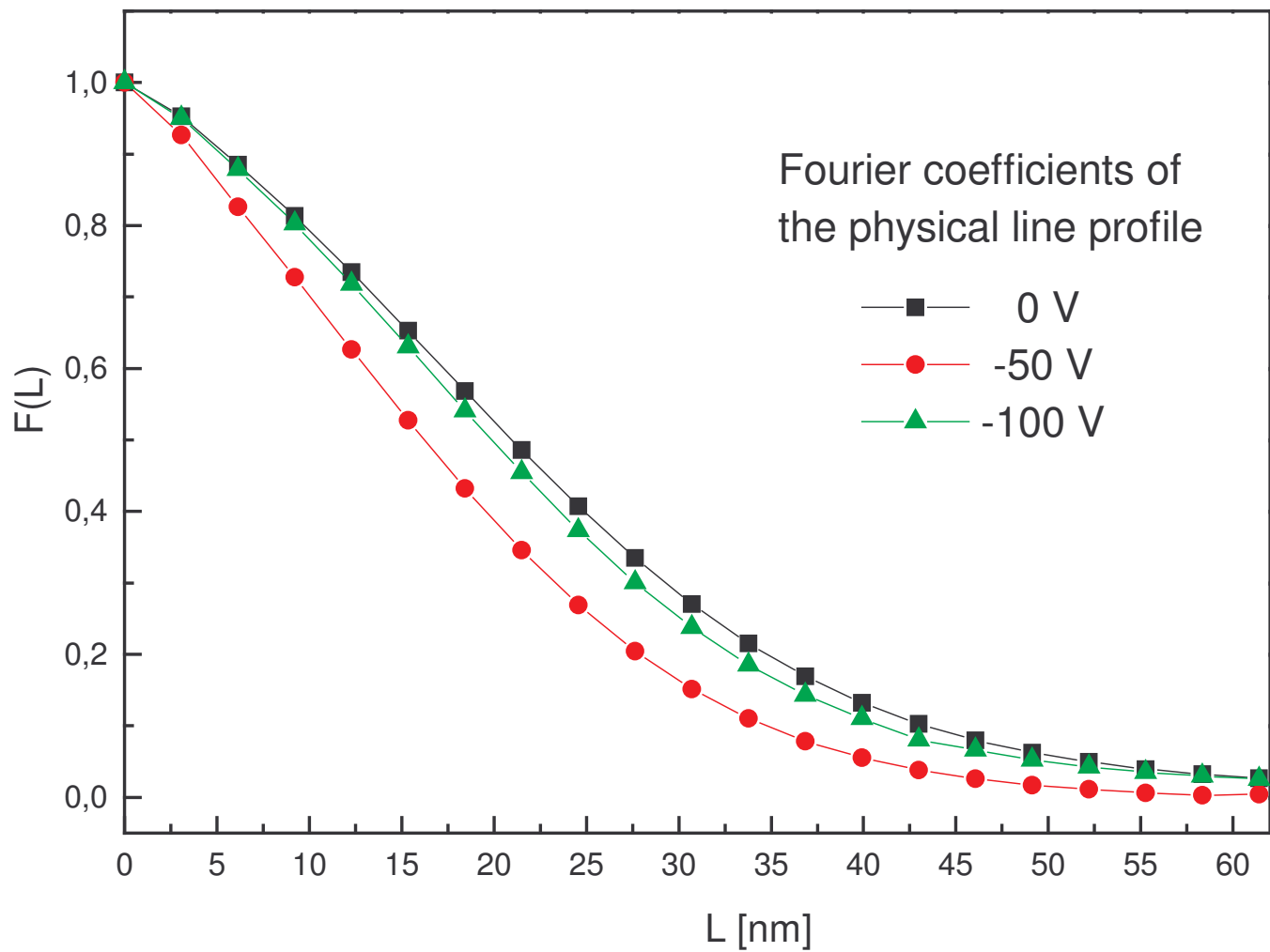
mittlere Versetzungsdichte

$$L_0$$

Abschneideradius (Spannungsfeld einer Versetzung)

$$\langle \varepsilon^2 \rangle = \langle \varepsilon^2(hkl) \rangle$$

mittlere quadratische Spannungen infolge von Defekten 2. Art



Fourier coefficients of the Indium(101) reflection for films deposited at different substrate voltages without oxygen flow

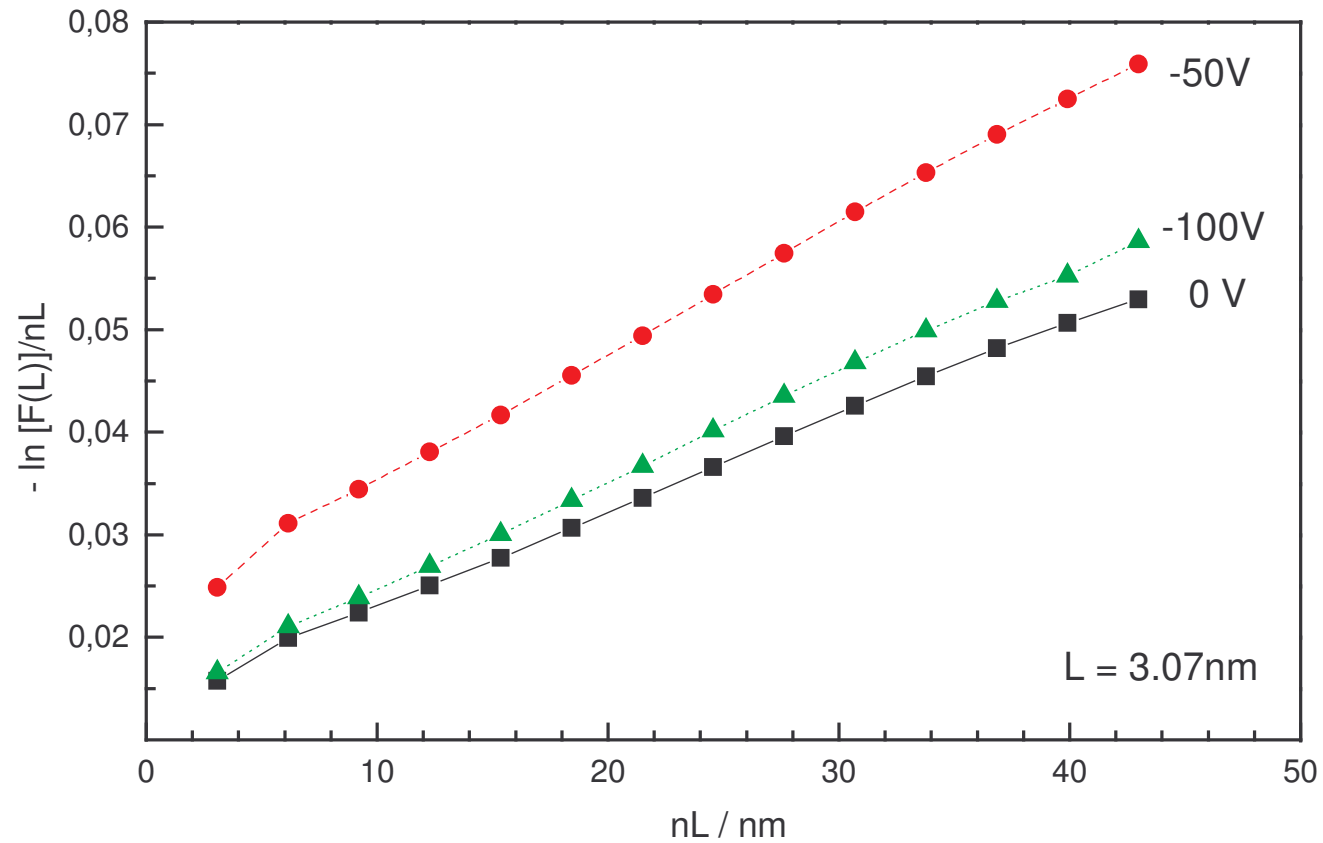
### **WARREN-AVERBACH-plot**

$$\gamma(L) = -\ln A(L)/L = 1/T + K \langle \varepsilon^2(L) \rangle L$$

### **KRIVOGLAZ-WILKENS-plot**

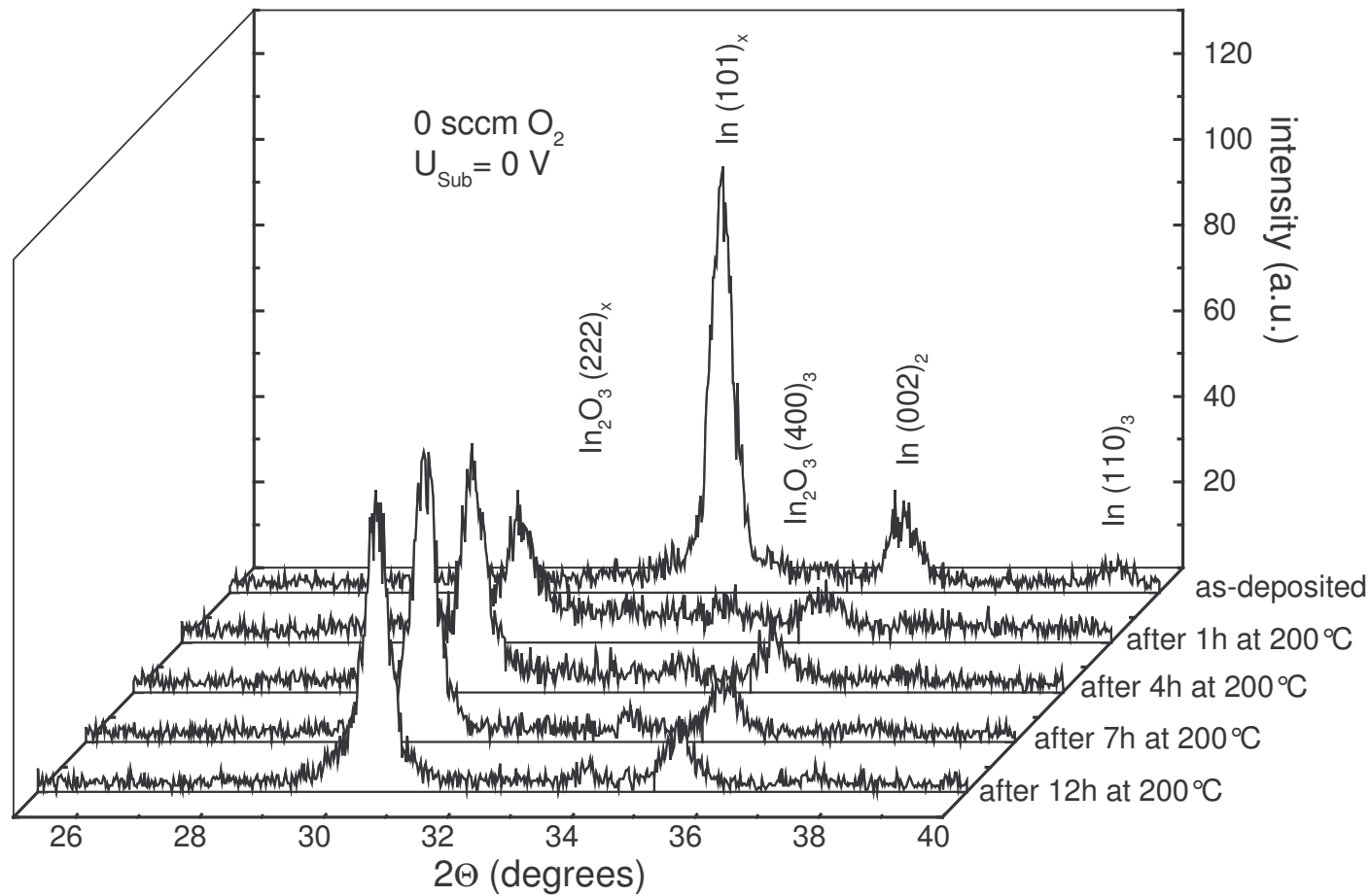
$$\psi(\ln L) = -\ln A(l)/L^2 = 1/TL + (K \langle \varepsilon^2 \rangle + B \ln L_0) - B \ln L$$

# WARREN-AVERBACH-plot für In(101)-Reflex

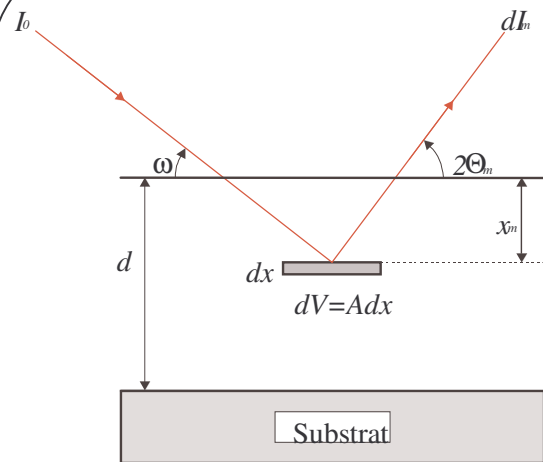


Physical parameters of In/Sn films  
deposited at various substrate voltages

$U_{\text{sub}}$	<b>0 V</b>	<b>-50 V</b>	<b>-100 V</b>
<b>T / nm</b>	74	43	71
$\langle \varepsilon^2 \rangle^{1/2}$	$1,87 \cdot 10^{-3}$	$2,14 \cdot 10^{-3}$	$1,98 \cdot 10^{-3}$
$\rho_V / \text{cm}^{-2}$	$0,56 \cdot 10^{-11}$	$1,10 \cdot 10^{-11}$	$0,64 \cdot 10^{-11}$
$d_{101} / \text{Å}$	2,7183	2,7142	2,71697
$\Delta V / \text{V}$	Referenz	-0,00455	-0,00149



Phase transformation of metallic In/Sn into crystalline ITO at  $200^\circ\text{C}$



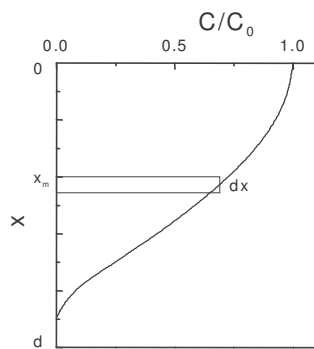
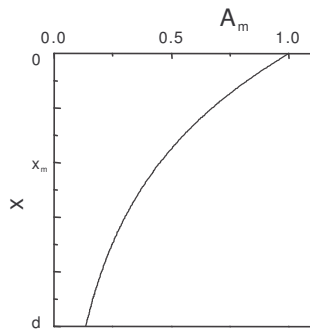
## Diffusion model

$$dI_m(t) = B_m K_0 I_0 A A_m C/C_0 dx \quad (1)$$

$$A_m = e^{-\bar{\mu}(x,t) z_m x_m} \quad (2)$$

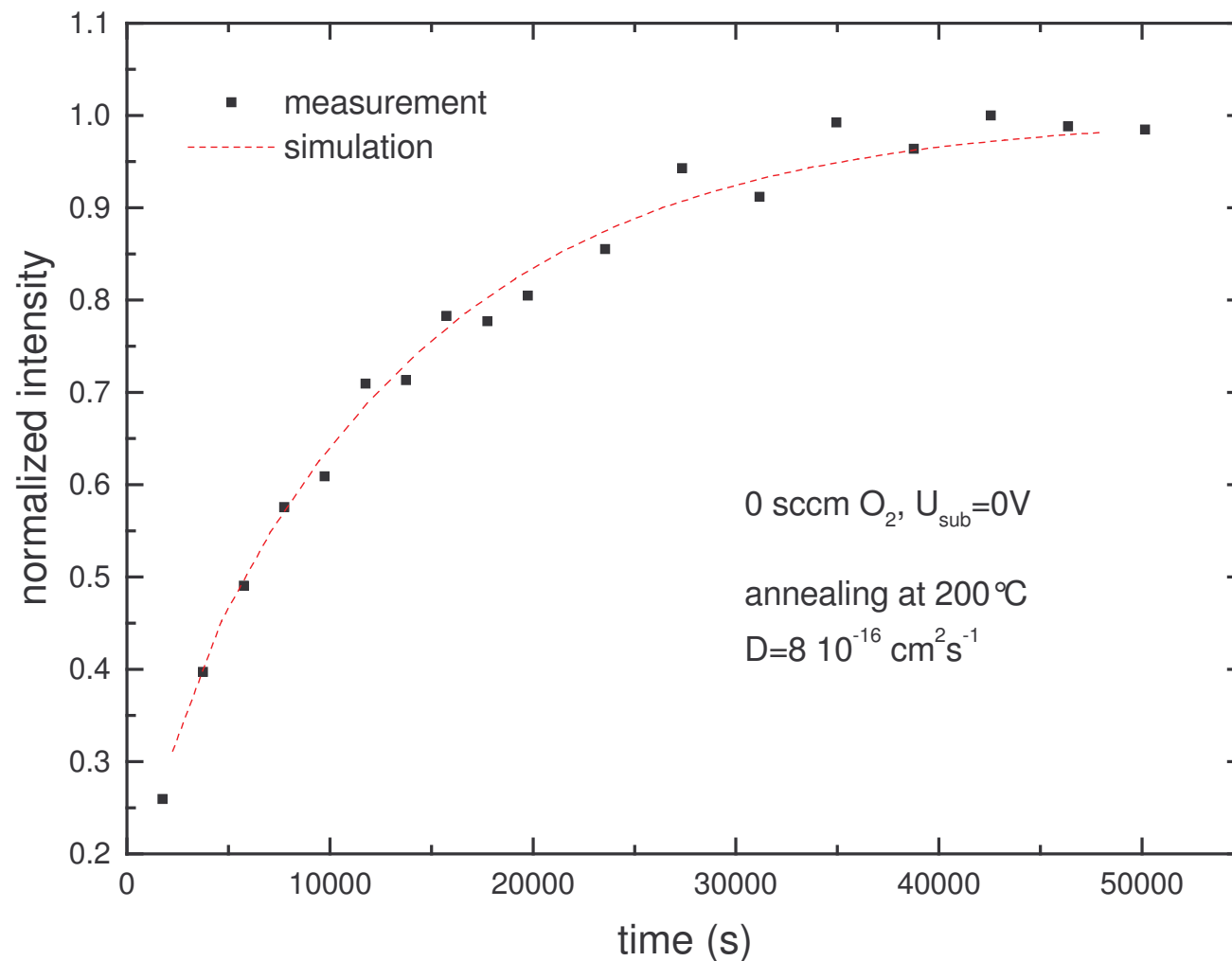
$$\bar{\mu} = \frac{1}{x_m} \int_0^{x_m} \mu dx = (\mu_m - \mu_n) \frac{1}{x_m} \int_0^{x_m} \left( f + (1-f) \frac{C^1}{C_0^1} \right) dx + \mu_n$$

$$\bar{\mu} = (\mu_m - \mu_n) f + (\mu_m - \mu_n)(1-f) \frac{1}{x_m} \int_0^{x_m} \frac{C^1}{C_0^1} dx + \mu_n.$$



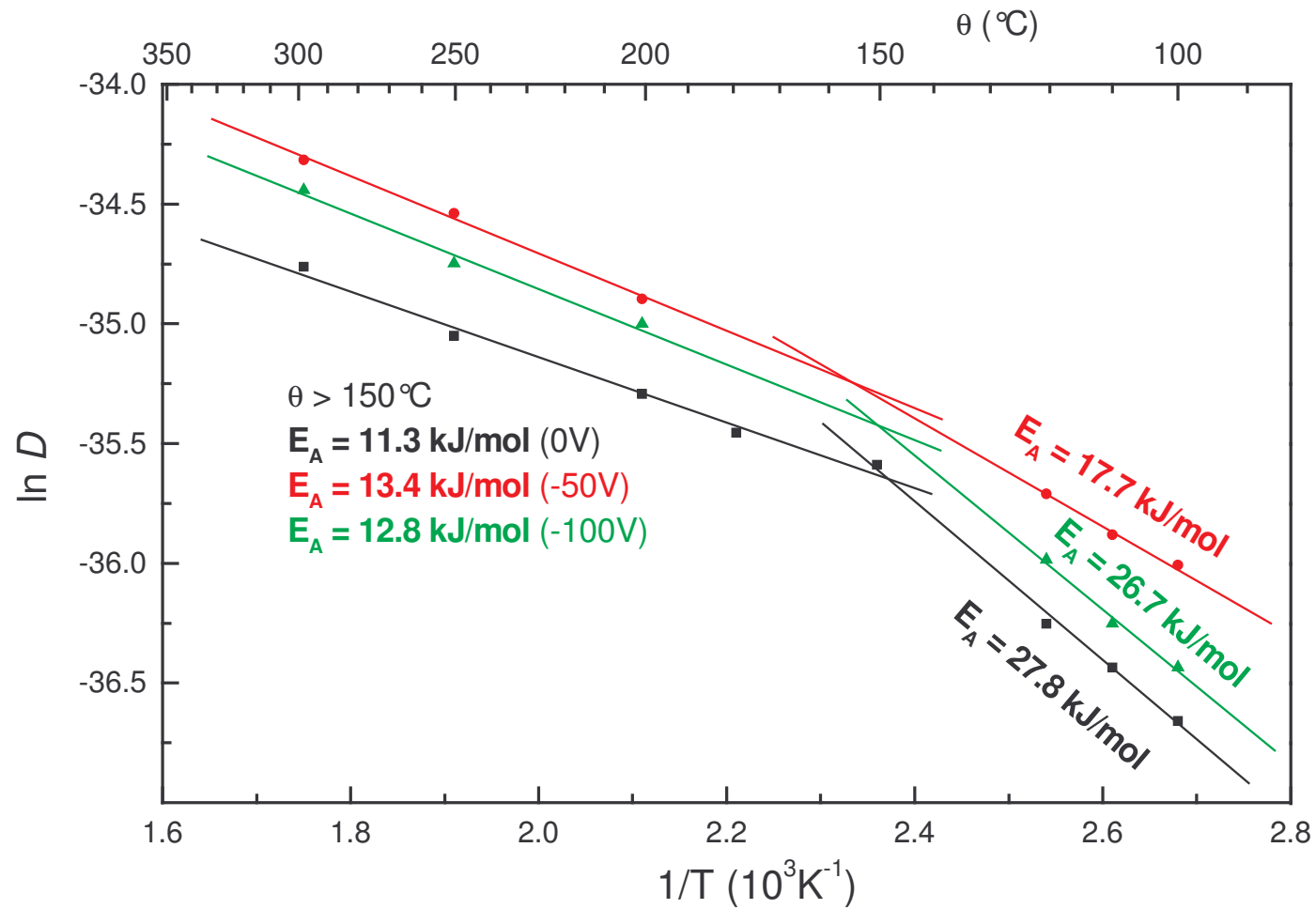
$$I_m(t) = B_m K_0 I_0 A \int_0^d C(x,t)/C_0 A_m dx \quad (3)$$

$$C(x,t)/C_0 = 1 - \frac{4}{\pi} \sum_{n=1}^{\infty} \frac{(-1)^{n-1}}{2n-1} \cdot \cos\left(\frac{2n-1}{2} \pi \frac{d-x}{d}\right) \cdot e^{-\left(\frac{2n-1}{2} \pi\right)^2 \frac{Dt}{d^2}} \quad (4)$$



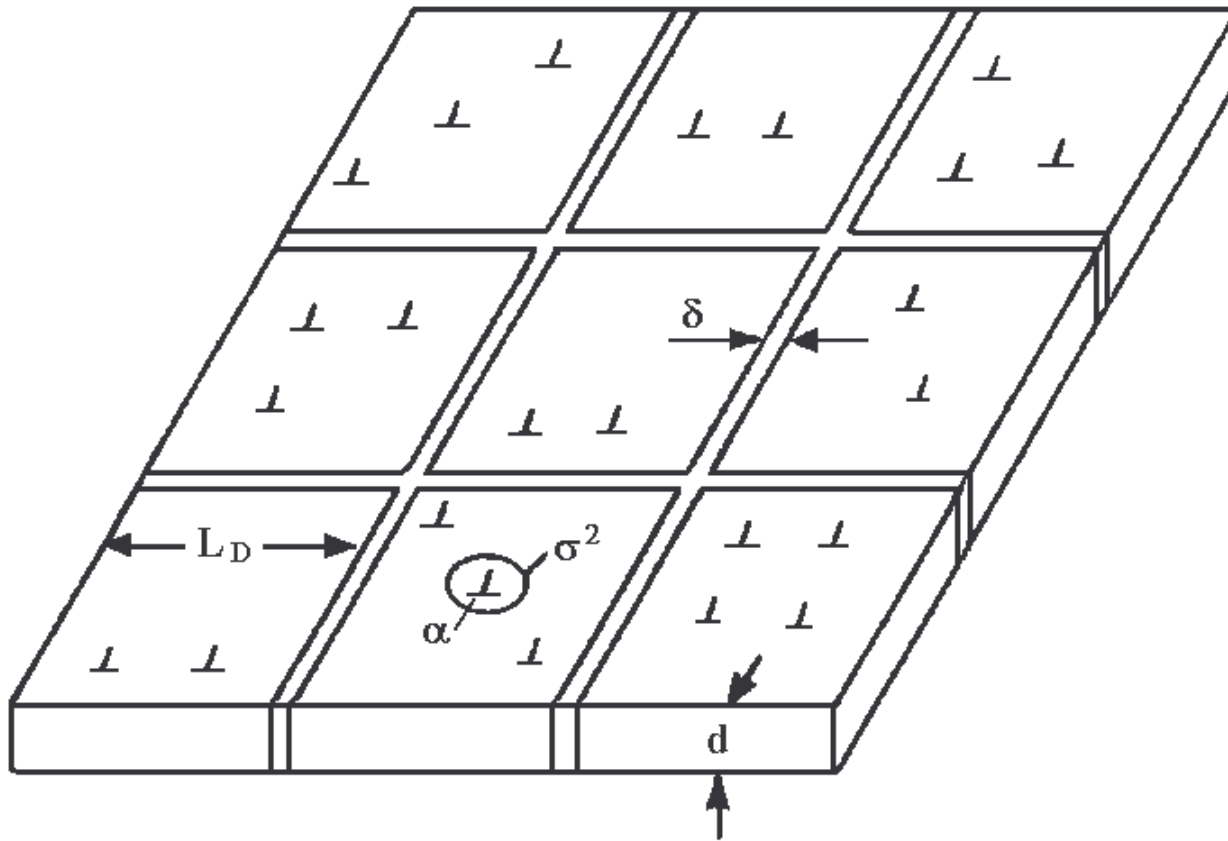
The measured normalized X-ray integral intensities ( $\hat{O}$ ) of ITO (222) reflection and the calculated intensity values (dashed line) versus time of a film deposited at 0 sccm O<sub>2</sub> and 0 V bias voltage

O <sub>2</sub> -flow / sccm	bias / V	D / 10 <sup>-16</sup> cm <sup>2</sup> s <sup>-1</sup>	f (amorphous ITO)
0	0	6	0
0.5		5.5	0.5
1.0		6	0.75
1.5		-	1
2.0		-	1
0	-50	13	0
0.5		17	0
1.0		14	0.3
1.5		15	0.5
2.0		16	0.7
0	-100	9.4	0
0.5		9.1	0
1.0		9.6	0.5
1.5		9.6	0.65
2.0		9.6	0.8



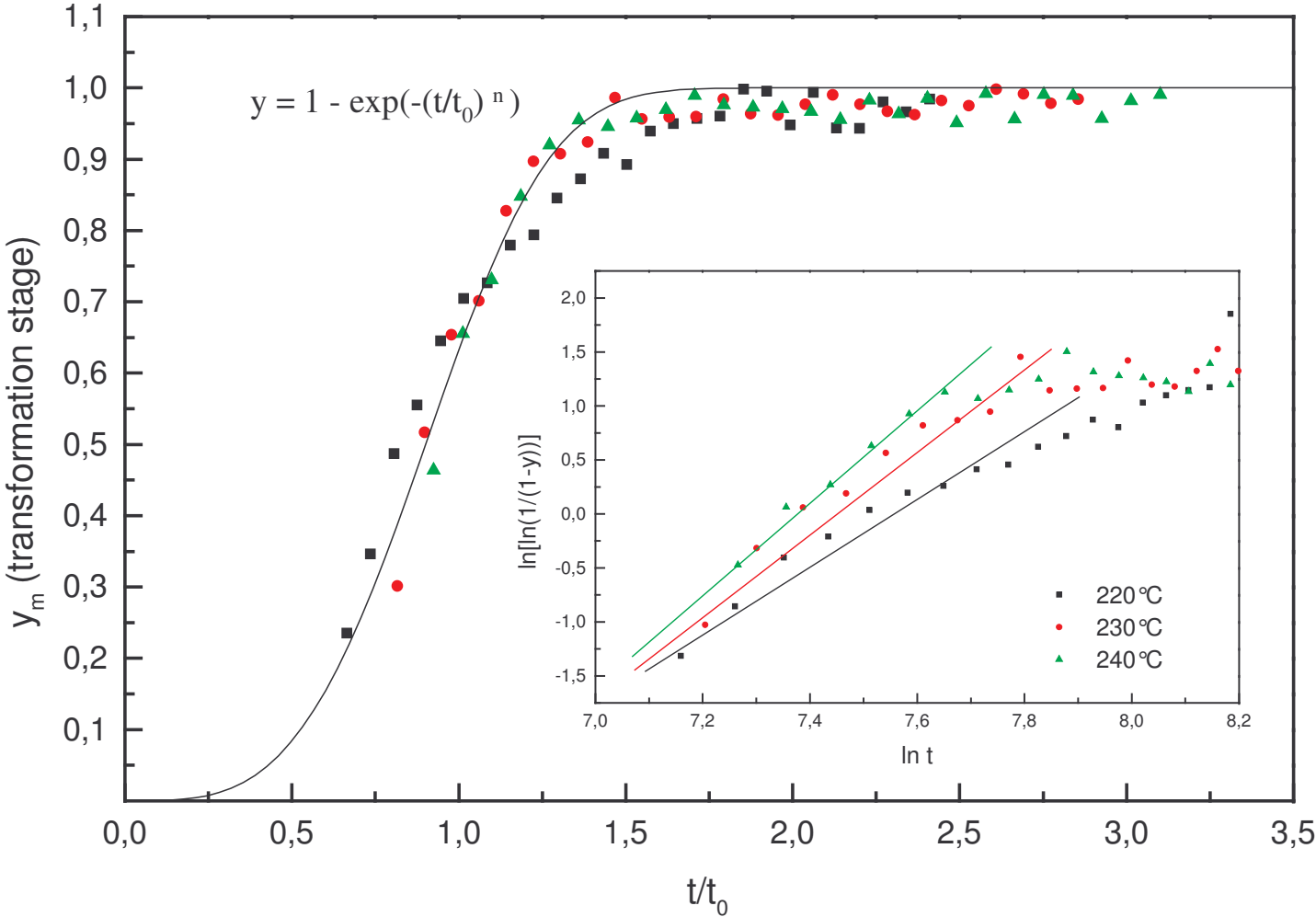
ARRHENIUS plot for the diffusion process: two different activation energies were found for  $T < 150^\circ\text{C}$  and  $T > 150^\circ\text{C}$

## „Highly idealized polycrystalline film“-Modell



$$D_{eff} = D_{vol} + \frac{\delta}{L_D} D_{KG} + \alpha \sigma^2 D_{vers}$$

# JOHNSON-MEHL-AVRAMI-plot für die Kristallisation amorphen ITO's



Target - In/Sn

Plasma

$\text{Ar}^+$ ,  $\text{Ar}^*$ ,  $\text{In}^+$ ,  $\text{In}^*$ ,  $\text{Sn}^+$ ,  $\text{Sn}^*$   
 $e^-$

0 V

-50 V

-100 V

In/Sn  
kristallin

In/Sn  
kristallin + Defekte

In/Sn  
kristallin + weniger  
Defekte

Target - In/In<sub>2</sub>O<sub>3</sub>

Plasma

Ar<sup>+</sup>, Ar<sup>\*</sup>, In<sup>+</sup>, In<sup>\*</sup>, In<sub>x</sub>O<sub>y</sub><sup>+</sup>, O<sup>+</sup>  
O<sub>2</sub><sup>-</sup>, O<sup>\*</sup>, e<sup>-</sup>, ???

0 V

-50 V

-100 V

